JVI Journals.ASM.org

Roles of Cell Signaling Pathways in Cell-to-Cell Contact-Mediated Epstein-Barr Virus Transmission

Asuka Nanbo,[a] Haruna Terada,[a]* Kunihiro Kachi,[a] Kenzo Takada,[b] and Tadashi Matsuda[a]

Graduate School of Pharmaceutical Sciences, Hokkaido University, Sapporo, Japan,[a] and Institute for Genetic Medicine, Hokkaido University, Sapporo, Japan[b]

Epstein-Barr virus (EBV), a human gamma herpesvirus, establishes a life-long latent infection in B lymphocytes and epithelial cells following primary infection. Several lines of evidence indicate that the efficiency of EBV infection in epithelial cells is accelerated up to 10^4-fold by coculturing with EBV-infected Burkitt's lymphoma (BL) cells compared to infection with cell-free virions, indicating that EBV infection into epithelial cells is mainly mediated via cell-to-cell contact. However, the molecular mechanisms involved in this pathway are poorly understood. Here, we establish a novel assay to assess cell-to-cell contact-mediated EBV transmission by coculturing an EBV-infected BL cell line with an EBV-negative epithelial cell line under stimulation for lytic cycle induction. By using this assay, we confirmed that EBV was transmitted from BL cells to epithelial cells via cell-to-cell contact but not via cell-to-cell fusion. The inhibitor treatments of extracellular signal-regulated kinase (ERK) and nuclear factor (NF)-κB pathways blocked EBV transmission in addition to lytic induction. The blockage of the phosphoinositide 3-kinase (PI3K) pathway impaired EBV transmission coupled with the inhibition of lytic induction. Knockdown of the RelA/p65 subunit of NF-κB reduced viral transmission. Moreover, these signaling pathways were activated in cocultured BL cells and in epithelial cells. Finally, we observed that viral replication was induced in cocultured BL cells. Taken together, our data suggest that cell-to-cell contact induces multiple cell signaling pathways in BL cells and epithelial cells, contributing to the induction of the viral lytic cycle in BL cells and the enhancement of viral transmission to epithelial cells.

Epstein-Barr virus (EBV), a human gamma herpesvirus, establishes a persistent latent infection in B lymphocytes and epithelial cells following primary infection (19). EBV has been implicated as a cause of lymphomas and epithelial malignancies, such as Burkitt's lymphoma (BL), Hodgkin's disease, nasopharyngeal carcinoma, and gastric cancer (19). EBV binds to B lymphocytes through a direct interaction of the EBV glycoprotein gp350/220 with the complement receptor CD21 (13, 22). In contrast, the mechanism by which EBV enters epithelial cells remains undefined. Epithelial cells express very low levels of CD21 or are CD21 negative in culture (12, 15), resulting in the lack of an efficient infection of cell-free viruses.

Several lines of evidence indicate that EBV infection into epithelial cells is mainly mediated by cell-to-cell contact (5, 15, 34, 35, 37, 43). The rate of EBV infection in epithelial cells increases up to 10^3-fold by coculturing with EBV-positive B cells compared to infection with cell-free EBV (5, 15, 43). Moreover, Shannon-Lowe et al. demonstrated that most EBV virions are retained on cell surfaces after binding to primary B cells and are transferred to epithelial cells, resulting in the 10^3- to 10^4-fold increase in infection compared to cell-free virus infection (35). All of these studies support a model in which EBV-infected B cells migrating into the epithelial stroma or intraepithelial space contribute to efficient EBV transmission into epithelium via cell-to-cell contact (42, 43). However, the molecular mechanisms of cell-to-cell EBV transmission remain unclear.

In the present study, we establish a novel assay to assess cell-to-cell contact-mediated EBV transmission by coculturing an EBV-infected BL cell line with an EBV-negative epithelial cell line under stimulation for lytic cycle induction in BL cells. By using this system, we showed that EBV transmission was mediated via cell-to-cell contact but not via cell-to-cell fusion. We demonstrated that the treatment of inhibitors of extracellular signal-regulated kinase (ERK) and nuclear factor (NF)-κB pathways blocked EBV transmission in addition to lytic induction. The blockage of the phosphoinositide 3-kinase (PI3K) pathway impaired EBV transmission coupled with the inhibition of lytic induction. Knockdown of the RelA/p65 subunit of NF-κB also reduced the efficiency of viral transmission. Moreover, these cell signaling molecules were activated in cocultured BL cells and epithelial cells. Finally, we observed that the viral lytic cycle was induced in BL cells by coculturing with epithelial cells. The possible roles of these signaling molecules in cell-to-cell contact-mediated EBV transmission are discussed.

MATERIALS AND METHODS

Cell culture. The African green monkey kidney epithelial Vero-E6 cell line (9, 26), which was provided by Ayato Takada, and human gastric adenocarcinoma cell lines, AGS (2, 49) and NU-GC-3 (1, 16, 22, 31, 32, 49), were grown in high-glucose Dulbecco's modified Eagle's medium (DMEM) containing 10% fetal bovine serum (FBS) and antibiotics. BL-derived Akata$^-$ EBV-eGFP cells, which are latently infected with a recombinant Akata strain of EBV carrying the enhanced green fluorescent protein (eGFP) gene inserted into the viral BXLF1 open reading frame (ORF) (22), were maintained in RPMI 1640 medium containing 10% FBS, antibiotics, and 800 μg/ml G418. EBV-positive BL-derived Akata (Akata$^+$) cells (39–41) and EBV-negative BL-derived Daudi (Daudi$^-$) cells (20, 28) were maintained in RPMI 1640 medium containing 10% FBS and antibiotics. Cells were maintained at 37°C in 5% CO_2.

Received 5 April 2012 Accepted 9 June 2012
Published ahead of print 20 June 2012
Address correspondence to Asuka Nanbo, nanboa@pharm.hokudai.ac.jp.
* Present address: RIKEN Wako Institute, Wako, Saitama, Japan.
A.N. and H.T. contributed equally to this work.

doi:10.1128/JVI.00712-12

EBV transmission assay. EBV-negative Vero-E6 cells (5×10^4) were cocultured with Akata$^-$ EBV-eGFP cells (5×10^5) for 24 h in 24-well plates in the presence or absence of 0.2% F(ab′)$_2$ fragments of goat anti-human IgG polyclonal antibody (αhIgG; Dako, Glostrup, Denmark) to induce the viral lytic cycle in Akata$^-$ EBV-eGFP cells. To remove Akata$^-$ EBV-eGFP, Vero-E6 cells were washed, trypsinized, and cultured in 6-well plates for 6 h in the absence of αhIgG. For the transmission assay with a physical barrier, Vero-E6 cells (1×10^5) were grown in the basolateral chamber of a 24-well plate with membrane inserts having pore sizes of 0.4 μm (Corning, Toledo, OH). Akata$^-$ EBV-eGFP cells (1×10^5) were added to the membrane inserts and incubated for 24 h in the presence or absence of αhIgG. Vero-E6 cells were grown on the coverslips and fixed in 4% paraformaldehyde (PFA). The transmission of EBV-eGFP into Vero-E6 cells was analyzed by a confocal laser scanning microscope (Fluoview FV10i; Olympus, Tokyo, Japan). Four fields containing approximately 2,000 cells were randomly collected, and the fractions of eGFP-positive Vero-E6 cells were measured. The percentages of eGFP-positive cells were also analyzed by flow cytometry (FACSCalibur, Becton, Dickinson and Company, Franklin Lakes, NJ). In parallel with fluorescence-activated cell sorting (FACS) analysis, the same sample was analyzed by a confocal laser scanning microscope to confirm that the sample did not contain Akata$^-$ EBV-eGFP cells.

Immunofluorescent staining. Vero-E6 cells were grown on coverslips and cocultured with Akata$^-$ EBV-eGFP cells under αhIgG treatment. For analysis of the expression of caveolin-1, EBNA1, and HLA-DR, Vero-E6 cells were washed to remove Akata$^-$ EBV-eGFP, cultured in 6-well plates for 6 h, and grown on coverslips. For analysis of the phosphorylation of ERK and PI3K and the nuclear translocation of RelA/p65, Vero-E6 cells grown in 35-mm glass-bottomed culture dishes (MatTek Corporation, Ashland, MA) were cocultured with Akata$^-$ EBV-eGFP cells in the presence or absence of 0.2% αhIgG for various times. The cells were fixed with 4% PFA in phosphate-buffered saline (PBS) for 10 min at room temperature, permeabilized with PBS containing 0.05% Triton X-100 for 10 min at room temperature, and blocked in PBS containing 1% bovine serum albumin (BSA) and 0.05% Triton X-100 for 20 min at room temperature. The cells were incubated with individual primary antibodies for 1 h at room temperature. After being washed twice in PBS, the cells were incubated with Alexa Fluor-labeled secondary antibodies (Life Technologies, Carlsbad, CA) for 1 h at room temperature. After being washed twice in PBS, the nucleus was counterstained with 4′,6-diamidino-2-phenylindole (DAPI). Images were collected with a 60× water objective lens (numeric aperture, 1.3) of a confocal laser scanning microscope (Fluoview FV10i) and acquired by using FV10-ASW software (Olympus). For presentation in the manuscript, all images were digitally processed with Adobe Photoshop. Rabbit polyclonal antibodies for human caveolin-1 and human RelA/p65 were purchased from Abcam (Cambridge, United Kingdom) and Santa Cruz Biotechnology (Santa Cruz, CA), respectively. Mouse monoclonal antibody for EBV-encoded EBNA1 and a phycoerythrin (PE)-labeled monoclonal antibody for human leukocyte antigen (HLA)-DR were provided by Hironori Yoshiyama (Hokkaido University) and Kenji Oritani (Osaka University), respectively. Rabbit monoclonal antibodies for phosphorylated ERK1/2 (The202/Tyr204) and Akt (Ser473) were purchased from Cell Signaling Technology (Danvers, MA). The percentages of signal-activated cells were analyzed by a confocal laser scanning microscope. Four fields containing approximately 1,000 cells were randomly collected, and the fractions of the activated cells were measured.

Flow cytometry. For analysis of FcR expression, Vero-E6 cells (5×10^5) or Akata$^+$ cells (5×10^5) were incubated with αhIgG (1:100) for 1 h on ice. The cells were washed twice in PBS and incubated with fluorescein isothiocyanate (FITC)-labeled rabbit anti-goat IgG (Sigma-Aldrich, St. Louis, MO) for 30 min on ice. After two washes in PBS, the binding of αhIgG was analyzed by flow cytometry. For analysis of the expression of EBV-encoded gp350, Vero-E6 cells were cocultured with Akata$^-$ EBV-eGFP cells in the presence or absence of 0.2% αhIgG. Akata$^-$ EBV-eGFP cells were harvested, fixed, permeabilized, and blocked as described above. The cells were incubated with anti-gp350 monoclonal antibody (C-1) (44) for 1 h at room temperature, washed twice in PBS, and incubated with Alexa Fluor 647-labeled secondary antibodies (Life Technologies). After being washed twice in PBS, the expression of gp350 was analyzed by flow cytometry.

Cell-free EBV infection. Akata$^-$ EBV-eGFP cells were treated with 0.2% αhIgG for 48 h for viral production. Vero-E6 or Daudi$^-$ cells (1×10^5) were incubated with culture supernatant of αhIgG-treated Akata$^-$ EBV-eGFP cells for 1 h at 37°C. The culture supernatant was replaced with fresh medium, and the cells were further incubated for 24 h. The cells were fixed with 4% PFA, and the infection efficiencies were analyzed by flow cytometry as described above.

Inhibitor treatment. Vero-E6 cells were cocultured with Akata$^-$ EBV-eGFP cells and treated with dimethylsulfoxide (DMSO), U0126 (Sigma-Aldrich), LY294002 hydrochloride (Cell Signaling Technology), wortmannin (Sigma-Aldrich), or BAY 11-7082 (Merck, Darmstadt, Germany) for 24 h in the presence or absence of 0.2% αhIgG. U0126, both LY294002 and wortmannin, and BAY11-7082 inhibit the ERK, PI3K, and NF-κB pathways, respectively. Vero-E6 cells were washed and cultured in 6-well plates for 6 h in the absence of αhIgG. The effect of these inhibitors on the transmission of EBV-eGFP into Vero-E6 cells was analyzed by flow cytometry as described for the EBV transmission assay. The effect of these inhibitors on the expression of gp350 in Akata$^-$ EBV-eGFP cells was analyzed by flow cytometry as described above.

Knockdown of RelA/p65 by shRNA. Vero-E6 cells (2×10^4) grown in 6-well plates were transfected by Fugene HG (Roche, Basel, Switzerland) with 3 μg of either pGPU6/GFP/Neo short hairpin RNA (shRNA) vector carrying two identical target sequences against the human RelA/p65 subunit of NF-κB (shRNA 1, GCCCATGGAATTCCAGTACCT; shRNA 2, GAATCCAGTGTGTGAAGAAGC) (Shanghai GenePharma, Shanghai, China) or pGPU6/GFP/Neo shRNA control plasmid possessing the target sequence against human glyceraldehyde-3-phosphate dehydrogenase (GAPDH) (GTATGACAACAGCCTCAAG) (Shanghai GenePharma). The individual G418-resistant cell clones were isolated, and the down-regulation of the RelA/p65 gene was analyzed by reverse transcription-PCR (RT-PCR) with sense (ATGGACGAACTGTTC) and antisense (TC CTTGGTGACCAGGG) oligonucleotides.

FISH. Fluorescent *in situ* hybridization (FISH) analysis was performed based on the protocol of Nanbo et al. (27), with some modifications. Briefly, Akata$^-$ EBV-eGFP cells were treated with 0.075 M KCl for 20 min at 37°C, fixed in methanol-acetic acid (3:1) for 30 min at room temperature, and spread on the slides. Slides were treated with 4× SSC (1× SSC is 0.15 M NaCl plus 0.015 M sodium citrate) containing 0.5% (vol/vol) Nonidet P-40 for 30 min at 37°C, dehydrated in a cold ethanol series (70, 80, and 90%) for 2 min each, air dried, and denatured in 70% formamide–2× SSC for 2 min at 72°C. Slides were dehydrated in a cold ethanol series and air dried. Hybridization probes for detection of EBV plasmids were generated by nick translation using biotin-11-dUTP (Roche). Twenty μg of a probe was precipitated by ethanol in the presence of 6 μg salmon sperm DNA (Eppendorf, Hamburg, Germany) and 4 μg human Cot-1 DNA (Life Technologies), resuspended in hybridization buffer (2× SSC, 50% formamide, 10% dextran sulfate), and incubated for 10 min at 70°C, for 5 min at 4°C, and for 1 h at 37°C. A hybridization mix containing 5 ng probe was placed on each sample and incubated overnight at 37°C in a moist chamber. Slides were washed in 2× SSC containing 50% formamide for 30 min at 50°C and in 2× SSC for 30 min at 50°C. After blocking in 4× SSC containing 1% BSA, the hybridized probe was revealed by incubation with streptavidin conjugated to Cy3 (Sigma-Aldrich) for 30 min at 37°C. Slides were washed twice in 4× SSC containing 0.05% Triton X-100 for 5 min at room temperature. The nucleus was counterstained with DAPI. The percentages of Akata$^-$ EBV-eGFP cells that underwent the lytic cycle were analyzed by a confocal laser scanning microscope. Four fields containing approximately 1,000 cells were randomly collected, and the fractions of the cells that underwent the lytic cycle were measured.

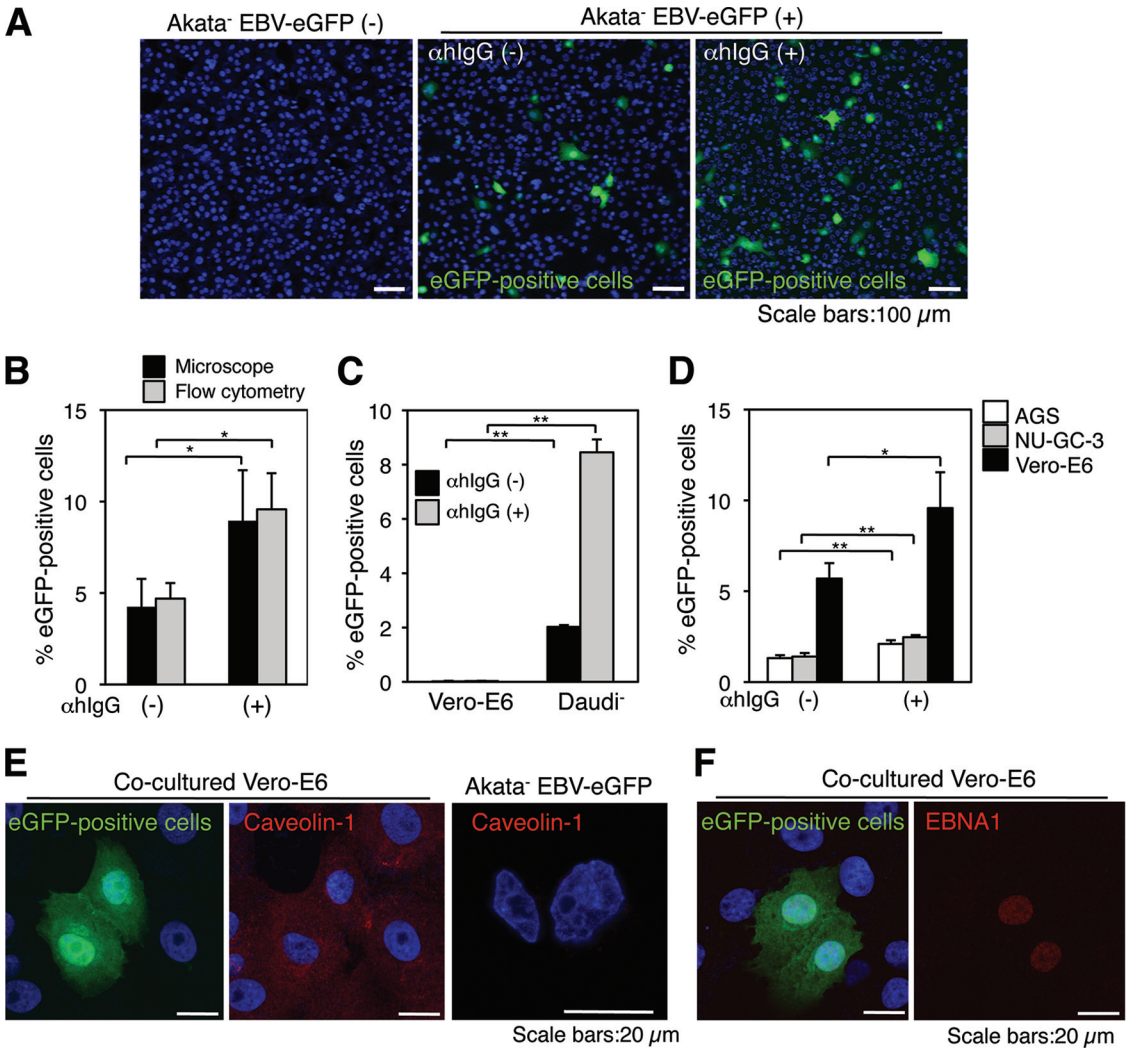

FIG 1 EBV is transmitted from BL cells to epithelial cells by cocultivation. (A) EBV transmission from BL cells to epithelial cells is facilitated by αhIgG treatment. Vero-E6 cells were cocultured with Akata$^-$ EBV-eGFP cells in the absence (middle) or presence (right) of αhIgG for 24 h. The infection of EBV-eGFP in Vero-E6 cells (green) was analyzed by a confocal laser scanning microscope. The left panel shows the result without cocultivation. The nucleus was counterstained with DAPI. Scale bars, 100 μm. (B) A summary of cell-to-cell contact-mediated EBV transmission. Vero-E6 cells were cocultured with Akata$^-$ EBV-eGFP cells in the absence or presence of αhIgG for 24 h. The percentages of EBV-eGFP-positive Vero-E6 cells were analyzed by a confocal laser scanning microscope (black bars) or flow cytometry (gray bars). The experiment was performed five times independently, and the averages and standard deviations are shown for each condition. *, $P < 0.05$ versus the respective control (Student's *t* test). (C) Infection of cell-free EBV-eGFP into Vero-E6 cells. Vero-E6 cells or Daudi$^-$ cells were incubated for 1 h at 37°C with culture supernatants derived from αhIgG-treated (gray bars) or untreated (black bars) Akata$^-$ EBV-eGFP cells. The culture supernatants were replaced with fresh medium, and the cells were further incubated for 48 h. The percentages of eGFP-positive cells were analyzed by flow cytometry. The experiment was performed three times independently. The averages and standard deviations are shown for each condition. **, $P < 0.01$ versus the respective control (Student's *t* test). (D) EBV-eGFP is transmitted to human gastric epithelial cells. AGS (white bars), NU-GC-3 (gray bars), or Vero-E6 (black bars) cells were cocultured with Akata$^-$ EBV-eGFP cells in the absence or presence of αhIgG for 24 h. The percentages of eGFP-positive epithelial cells were analyzed by flow cytometry. The experiment was performed three times independently, and the averages and standard deviations are shown for each condition. *, $P < 0.05$ versus the respective control. **, $P < 0.01$ versus the respective control (Student's *t* test). (E) EBV-eGFP is transmitted to Vero-E6 cells. Vero-E6 cells were cocultured with Akata$^-$ EBV-eGFP cells under the treatment of αhIgG for 24 h. The expression of an epithelium marker, caveolin-1, was analyzed by immunofluorescent staining. Caveolin-1 (red; middle) was expressed in eGFP-positive cells (green; left); BL-derived Akata$^-$ EBV-eGFP cells were caveolin-1 negative (right). The nucleus was counterstained with DAPI. Scale bars, 20 μm. (F) eGFP-positive Vero-E6 cells are infected with EBV-eGFP. Vero-E6 cells were cocultured with Akata$^-$ EBV-eGFP cells under treatment with αhIgG for 24 h. The expression of EBV-encoded nuclear antigen 1 (EBNA1) was analyzed by immunofluorescent staining. eGFP-positive Vero-E6 cells (green; left) were EBNA1 positive (red; right). The nucleus was counterstained with DAPI. Scale bars, 20 μm.

RESULTS

EBV is transmitted from cocultured BL cells to epithelial cells. We established a cocultivation system to evaluate the efficiency of cell-to-cell EBV transmission. We cocultured EBV-negative African green monkey kidney epithelial Vero-E6 cells (9, 26) with BL-derived Akata$^-$ EBV-eGFP cells, which are latently infected with a recombinant Akata strain of EBV the encoding eGFP gene inserted into the viral genome (22) for 24 h. To amplify viral transmission, we cross-linked the cell surface IgG of Akata$^-$ EBV-eGFP by adding F(ab′)$_2$ fragments of goat anti-human IgG polyclonal antibody (αhIgG) to induce the viral lytic cycle (39–41). The transmission of EBV-eGFP to Vero-E6 cells was analyzed by a

confocal laser scanning microscope (Fig. 1A and B, black bars) and flow cytometry (Fig. 1B, gray bars). EBV-eGFP infected approximately 5% of the cell population by coculturing with Akata$^-$ EBV-eGFP (Fig. 1A, left and middle, and B). αhIgG treatment increased the transmission rate to 9% (Fig. 1A, right, and B).

We also examined the infection efficiency of cell-free virus into Vero-E6 cells. We treated Akata$^-$ EBV-eGFP cells with αhIgG for 48 h for the production of EBV-eGFP. Vero-E6 cells or EBV-negative BL-derived Daudi$^-$ cells (20, 28) were incubated with the culture supernatant of αhIgG-treated Akata$^-$ EBV-eGFP cells, and the percentages of eGFP-positive cells were analyzed by flow cytometry. The cell-free virus infected Daudi$^-$ cells efficiently (Fig. 1C). In contrast, Vero-E6 cells were highly resistant to cell-free viral infection (Fig. 1C).

We also examined the efficiency of EBV transmission into two human gastric epithelial cell lines, AGS (2, 49) and NU-GC-3 (1, 16, 22, 31, 32, 49). EBV-eGFP was also transmitted to AGS (Fig. 1D, white bars) and NU-GC-3 cells (Fig. 1D, gray bars) in the absence (1.4 and 1.8%, respectively) and in the presence (2.3 and 2.4%, respectively) of αhIgG (Fig. 1D). Because EBV-eGFP was transmitted into Vero-E6 cells more efficiently, we used Vero-E6 cells for further study. We confirmed that eGFP-positive cells expressed an epithelial marker, caveolin-1 (7) (Fig. 1E, left and middle). All eGFP-positive cells expressed EBV-encoded nuclear antigen 1 (EBNA1) (Fig. 1F), indicating that the expressed eGFP in Vero-E6 cells was derived from incoming EBV-eGFP.

Flow-cytometric analysis demonstrated that αhIgG bound to the surface of Vero-E6 cells with low efficiency, suggesting that Vero-E6 cells express low levels of Fc receptor (FcR) (Fig. 2A, left, and B). It is possible that αhIgG-mediated cross-linking of the FcR of Vero-E6 cells initiates cellular signaling pathways and affects viral transmission. A previous study demonstrated that certain anti-IgG antibodies coat particles of measles virus and enhance viral entry into monocytes and macrophages (14), suggesting that αhIgG treatment enhances EBV infection of Vero-E6 cells in a similar way. To test these possibilities, we treated Akata$^-$ EBV-eGFP cells with αhIgG for 2 h, replaced the culture medium with fresh medium to remove free αhIgG, and cocultured Akata$^-$ EBV-eGFP cells with Vero-E6 cells for an additional 24 h. EBV was transmitted similarly in the presence and absence of free αhIgG (Fig. 2C), indicating that αhIgG-induced enhancement of viral transmission was independent of αhIgG-coated virions and cross-linking of FcR of Vero-E6 cells.

EBV is transmitted from BL cells to epithelial cells via cell-to-cell contact. We further examined whether viral transmission requires physical contact. Vero-E6 cells were grown on the basolateral chamber of transculture plates with membrane inserts having pore sizes of 0.4 μm. Akata$^-$ EBV-eGFP cells were added to the inserts and incubated for 24 h in the presence or absence of αhIgG. We analyzed the titer of eGFP-EBV in the culture supernatant of the basolateral chamber released from the insert containing αhIgG-treated Akata$^-$ eGFP EBV cells by incubating the culture supernatant with Daudi$^-$ cells. We confirmed that 38% of released eGFP-EBV was transferred to the basolateral chambers through the membrane (data not shown). Viral transmission did not occur if physical cell-to-cell contact was impaired (Fig. 3A, left and middle, and B), indicating that physical contact is indispensable for efficient viral transmission to epithelial cells.

The EBV lytic cycle induces the expression of the viral glycoproteins, which possess membrane fusion activity (6, 24, 33). To test the possibility that these surface glycoproteins mediate the fusion of plasma membranes between Akata$^-$ EBV-eGFP cells and Vero-E6 cells and thus the transfer of virus and/or eGFP to Vero-E6 cells, we assessed the expression of HLA-DR in eGFP-positive Vero-E6 cells by immunofluorescent staining. HLA-DR is the class II histocompatibility molecule constitutively expressed on antigen-presenting cells, including B cells, and T lymphocytes only after activation (45). We confirmed that Akata$^-$ EBV-eGFP cells expressed HLA-DR and that Vero-E6 cells are HLA-DR negative (Fig. 3C). All eGFP-expressing Vero-E6 cells were HLA-DR negative (Fig. 3C), indicating that EBV-eGFP transmission was mediated via cell-to-cell contact but not via cell-to-cell fusion.

The effect of inhibitors of cell signaling pathways on cell-to-cell contact-mediated EBV transmission. Because the molecular mechanism of cell-to-cell EBV transmission remains undefined, we investigated the roles of cellular signaling pathways in this process by using specific inhibitors. We cocultured Vero-E6 cells with Akata$^-$ EBV-eGFP cells in the presence and absence of αhIgG under the treatment of inhibitors such as U0126, LY294002, wortmannin, and BAY11-7082. U0126, both LY294002 and wortman-

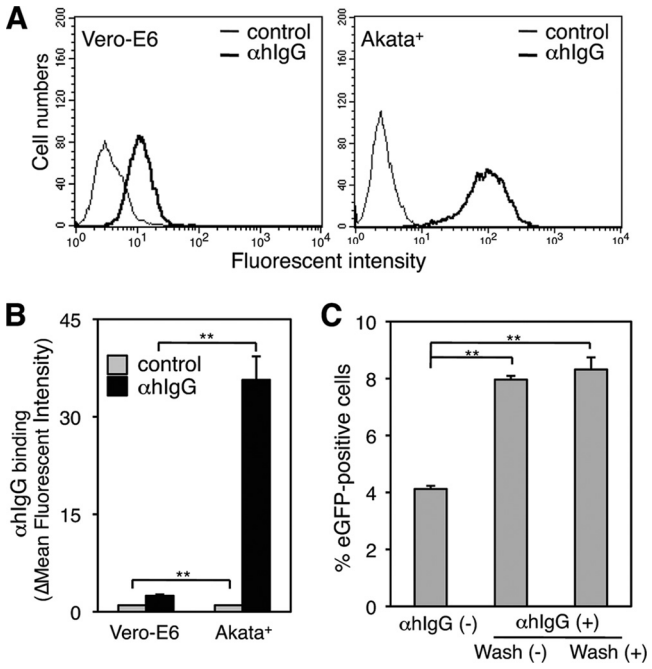

FIG 2 Role of free αhIgG in viral transmission. (A) The binding of αhIgG to Vero-E6. Vero-E6 cells (left) or Akata$^+$ cells (right) were incubated with 0.1% αhIgG on ice. The binding of αhIgG was revealed with FITC-labeled secondary antibody (boldface lines) by flow cytometry. As a control, cells were incubated with the secondary antibody (thin lines). (B) Summary of binding of αhIgG. The efficiency of binding of αhIgG to Vero-E6 or Akata$^+$ cells was quantified by flow cytometry (black bars). As a control, cells were incubated with the secondary antibody (gray bars). The experiment was performed three times independently, and the averages and standard deviations are shown for each condition. **, $P < 0.01$ versus the respective control (Student's *t* test). (C) The role of free αhIgG in viral transmission. Akata$^-$ EBV-eGFP cells were treated with αhIgG for 2 h, washed to remove free αhIgG, and cocultured with Vero-E6 cells for 24 h. The percentage of eGFP-positive epithelial cells was analyzed by flow cytometry. As a control, Akata$^-$ EBV-eGFP cells were cocultured with Vero-E6 cells in the presence of free αhIgG. The experiment was performed three times independently, and the averages and standard deviations are shown for each condition. **, $P < 0.01$ versus the respective control (Student's *t* test).

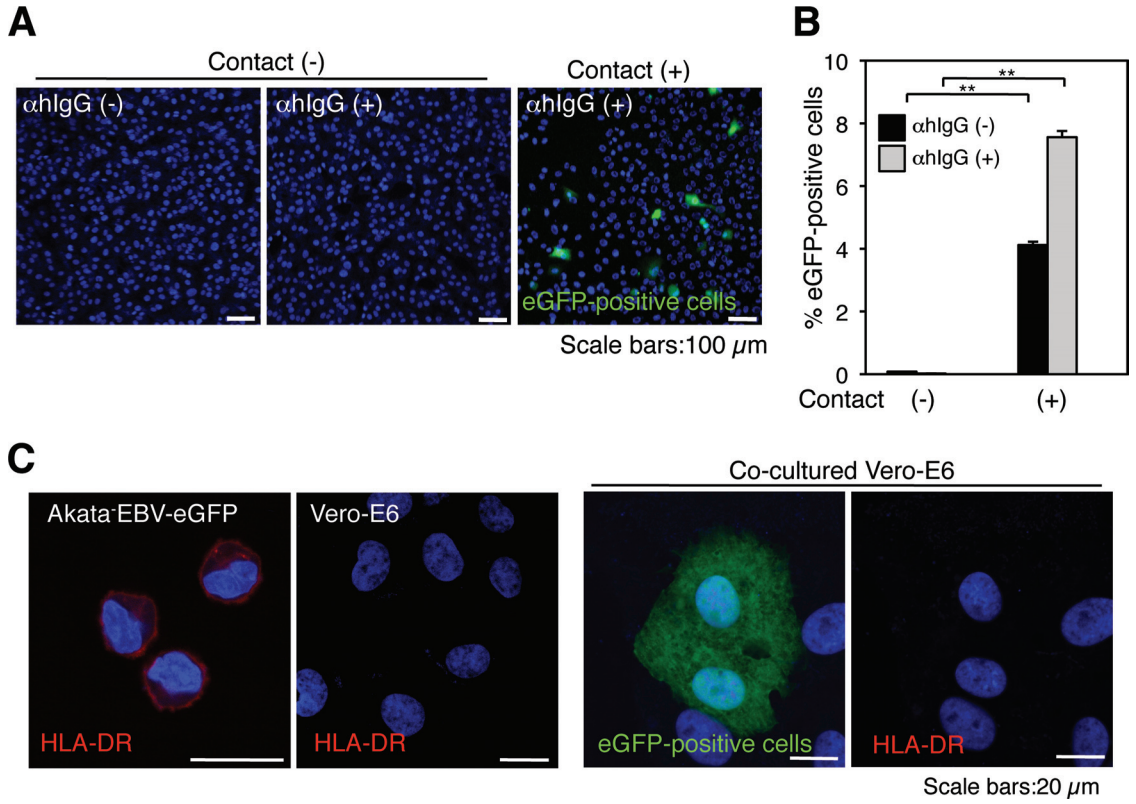

FIG 3 EBV is transmitted from BL cells to epithelial cells via cell-to-cell contact. (A) Physical cell-to-cell contact is required for EBV transmission. Vero-E6 cells were grown in the basolateral chamber of transculture inserts with pore sizes of 0.4 μm. Akata$^-$ EBV-eGFP cells were added to the inserts and incubated in the presence (left) or absence (middle) of αhIgG for 24 h. As a control, Vero-E6 cells were cocultured with Akata$^-$ EBV-eGFP in the presence of αhIgG (right). The infection of EBV-eGFP into Vero-E6 (green) was analyzed by a confocal laser scanning microscope. The nucleus was counterstained with DAPI. Scale bars, 100 μm. (B) A summary of viral transmission with a physical barrier. Vero-E6 cells were grown in the basolateral chamber of transculture plates. Akata$^-$ EBV-eGFP cells were added to the inserts and incubated in the presence (gray bars) or absence (black bars) of αhIgG for 24 h. As a control, Vero-E6 cells were cocultured with Akata$^-$ EBV-eGFP in the presence (gray bars) or absence (black bars) of αhIgG. The infection of EBV-eGFP in Vero-E6 cells was analyzed by flow cytometry. The experiment was performed three times independently. The averages and standard deviations are shown for each condition. **, $P < 0.01$ versus the respective control (Student's *t* test). (C) EBV transmits from BL cells to epithelial cells via cell-to-cell contact. Akata$^-$ EBV-eGFP cells were cocultured with Vero-E6 cells in the presence of αhIgG for 24 h. The expression of HLA-DR (red) in Akata$^-$ EBV-eGFP or Vero-E6 cells was analyzed by immunofluorescent staining (left panels). HLA-DR (red) was expressed in eGFP-positive Vero-E6 cells (green) (right panels). The nucleus was counterstained with DAPI. Scale bars, 20 μm.

nin, and BAY11-7082 inhibit the ERK (11), PI3K (46), and NF-κB pathways (50), respectively. We treated the cells with these inhibitors in various concentrations that did not exhibit cytotoxicity. αhIgG treatment triggers a variety of signaling pathways concurrent with induction of the lytic cycle (36). To exclude the possibility that the inhibitors reduced αhIgG-induced viral production, we also measured the effect of these inhibitors on the expression of viral lytic gene gp350 (22, 30) by flow-cytometric analysis. The expression of gp350 was enhanced under treatment with αhIgG (Fig. 4A, bottom). U0126 and BAY11-7082 significantly inhibited cell-to-cell contact-mediated EBV transmission (Fig. 4A, top) with moderate impairment of gp350 expression (Fig. 4A, bottom), suggesting that the ERK and the NF-κB pathways contribute to EBV transmission in addition to lytic induction. Both PI3K inhibitors, LY294002 and wortmannin, blocked EBV transmission and gp350 expression similarly (Fig. 4A), suggesting that the blockage of the PI3K pathway impaired EBV transmission coupled with inhibition of the lytic induction.

We further examined the role of the NF-κB pathway in cell-to-cell contact-mediated EBV transmission by using shRNA targeting the RelA/p65 subunit of NF-κB in Vero-E6 cells (Fig. 4B). The knockdown of RelA/p65 significantly reduced viral transmission (Fig. 4C). Taken together, the NF-κB pathway contributes to EBV transmission and moderately to the viral lytic cycle. The inhibitor treatments and knockdown of RelA/p65 also reduced viral transmission and lytic induction in the absence of αhIgG (Fig. 4A and C).

Cell signaling molecules activate immediately in the cocultivated cells. Because specific inhibitors of the ERK, PI3K, and NF-κB pathways significantly blocked cell-to-cell contact-mediated EBV transmission, we examined whether these signaling molecules are activated in cocultured BL cells and epithelial cells. We assessed the status of the ERK, PI3K, and NF-κB signaling pathways by immunofluorescent staining in Akata$^-$ EBV-eGFP cells and Vero-E6 cells, respectively. By using a laser scanning confocal microscope, we confirmed that the individual marker proteins in Akata$^-$ EBV-eGFP cells (HLA-DR) and Vero-E6 cells (caveolin-1) were detected without leakage of the signal derived from cocultured cells (Fig. 5A).

Under stimulation of the ERK pathway, the activation loop residues Thr202/Tyr204 and Thr185/Tyr187 of ERK are phosphorylated by a sequential protein kinase cascade (3). We ana-

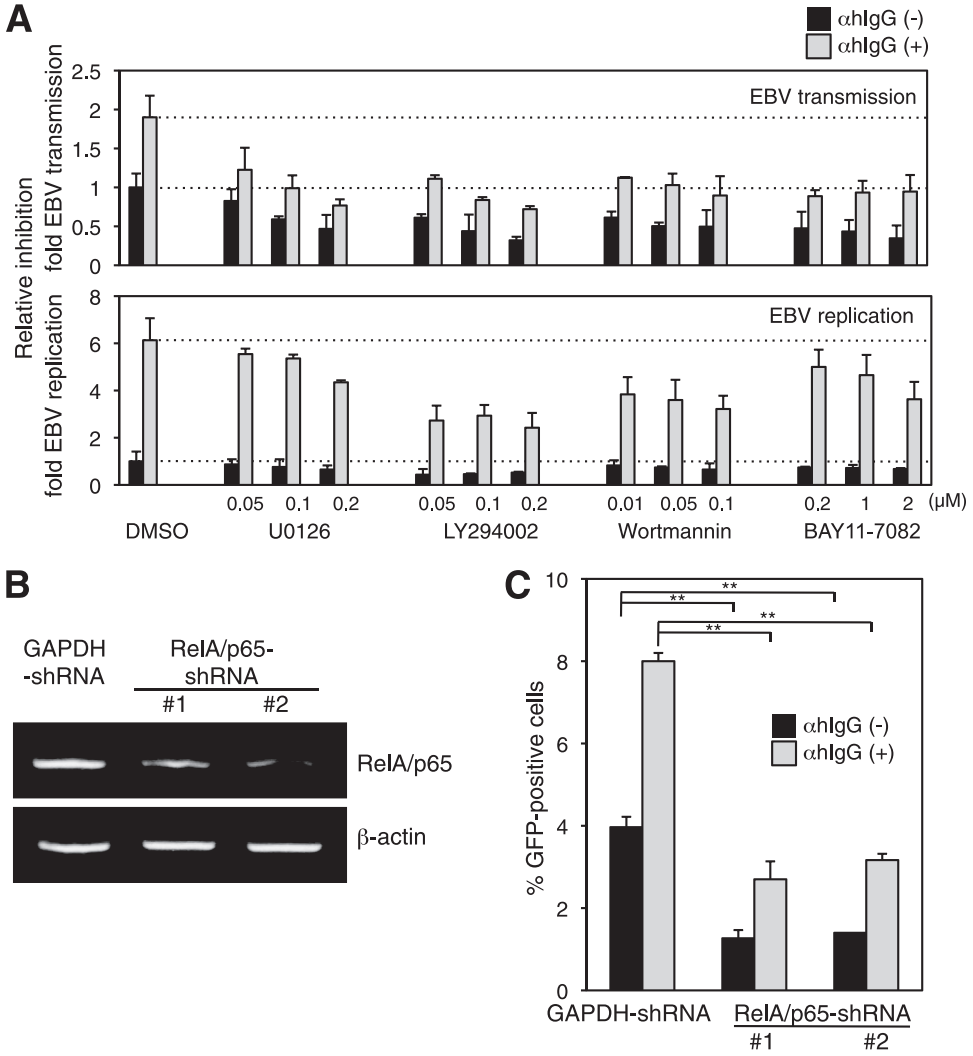

FIG 4 Effect of the inhibitors of cell signaling pathways on cell-to-cell contact-mediated EBV transmission and replication. (A) The effect of the inhibitors on cell-to-cell contact-mediated EBV transmission (top) and EBV replication (bottom). Vero-E6 cells were cocultured with Akata$^-$ EBV-eGFP cells in the presence (gray bars) or absence (black bars) of αhIgG under treatment with DMSO, U0126, LY294002, wortmannin, or BAY11-7082 for 24 h. The percentages of eGFP-positive cells were analyzed by flow cytometry. The data were normalized to untreated and DMSO-treated cells (top). Cocultured Akata$^-$ EBV-eGFP cells were harvested, and the expression of gp350 was analyzed by flow cytometry. The data were normalized to αhIgG-untreated and DMSO-treated cells (bottom). The experiment was performed three times independently. The averages and standard deviations are shown for each condition. (B) RelA/p65 knockdown by shRNA in Vero-E6 cells. Total RNA was isolated from two Vero-E6 clones stably expressing shRNA against human NF-κB RelA/p65 (RelA/p65-shRNAs 1 and 2) and a control expressing shRNA against human glyceraldehyde-3-phosphate dehydrogenase (GAPDH-shRNA). Knockdown of RelA/p65 mRNA was analyzed by RT-PCR (top). As a control, the expression of β-actin mRNA is shown (bottom). (C) The effect of RelA/p65 knockdown on cell-to-cell contact-mediated EBV transmission. RelA/p65-shRNA or GAPDH-shRNA was cocultured with Akata$^-$ EBV-eGFP cells in the presence (gray bars) or absence (black bars) of αhIgG for 24 h. Viral transmission was assessed by flow cytometry. The experiment was performed three times independently. The averages and standard deviations are shown for each condition. **, $P < 0.01$ versus the respective control (Student's *t* test).

lyzed the phosphorylation status of ERK by immunofluorescent staining. Phosphorylated ERK was observed diffusely in the cytoplasm in both Akata$^-$ EBV-eGFP cells (Fig. 5B and D) and Vero-E6 cells (Fig. 5C and D) 30 min after cocultivation. The phosphorylation was transient and disappeared 3 h and 30 min after cocultivation in Alata-EBV-eGFP and Vero-E6 cells, respectively (Fig. 5B to D).

To analyze the activation of the PI3K pathway, we assessed the level of phospho-Ser473 of Akt, which is a key component of the pathway (21). The phosphorylated Akt was distributed in the plasma membrane of Akata$^-$ EBV-eGFP cells 1 h after cocultivation, and the activation continued stably (Fig. 6A and C). Akt was transiently phosphorylated in the cytoplasm of Vero-E6 cells 1 h after cocultivation (Fig. 6B and C).

Following stimulation of the NF-κB pathway, the inhibitor of kB (IKB) inhibitory subunit of the NF-κB complex is phosphorylated, ubiquitinated, and degraded, and the transcription factor subunits of the NF-κB complex subunit (RelA/p65 and RelA/p50) translocate into the nucleus, resulting in the modulation of gene transcription (23). Because its nuclear import is a key event in NF-κB activation, we assessed the distribution of the RelA/p65 subunit in cocultured cells by immunofluorescent staining. RelA/p65 transiently translocated to the nucleus in cocultured Vero-E6 cells (Fig. 7B and C). In contrast, RelA/p65 translocated to the

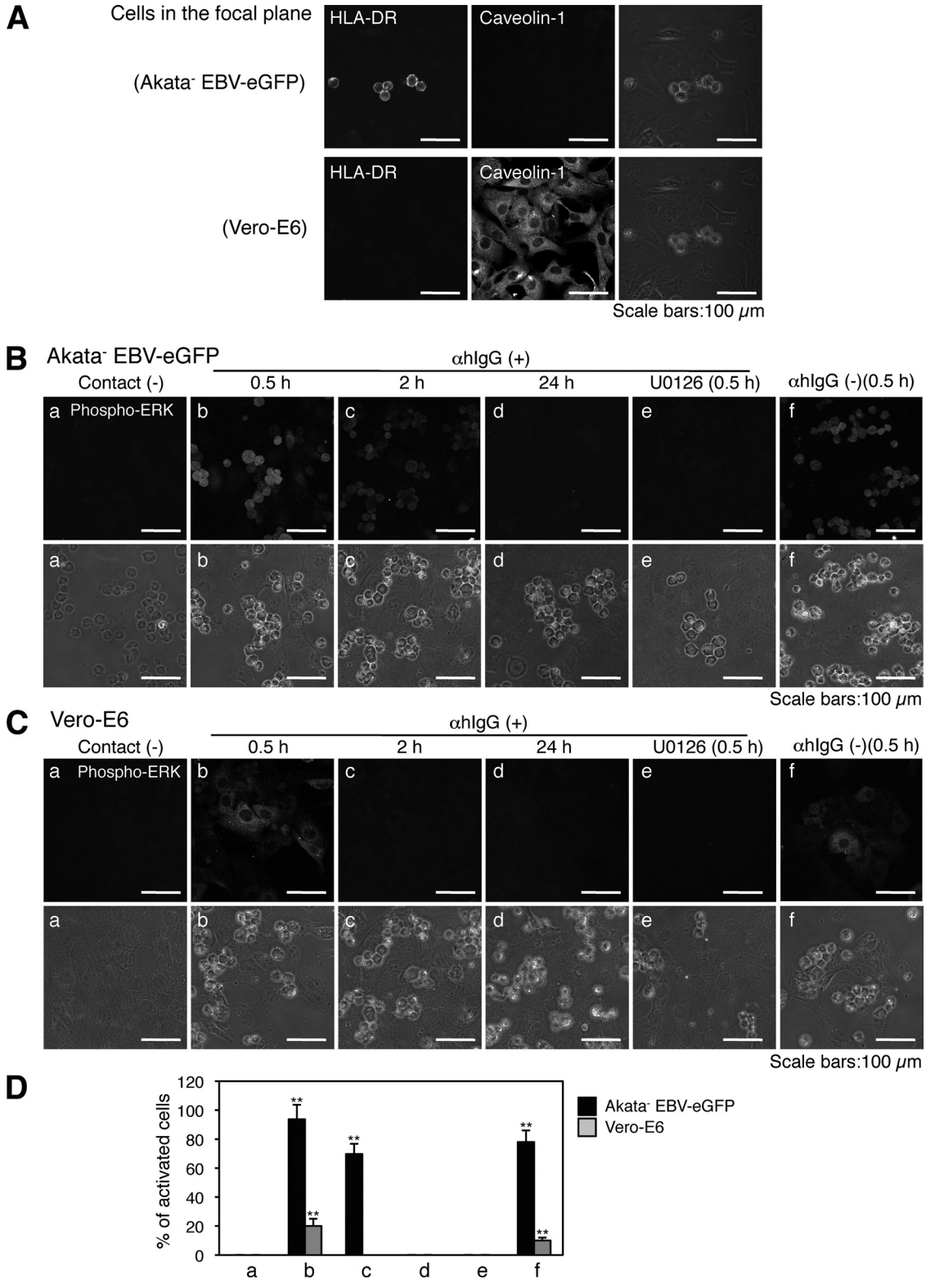

FIG 5 Activation of the ERK pathway in cocultured cells. (A) Immunofluorescent staining analysis in cocultured cells. Vero-E6 cells grown in 35-mm glass-bottomed culture dishes were cocultured with Akata$^-$ EBV-eGFP cells for 4 h. The cells were harvested and subjected to immunofluorescent staining to analyze the expression of HLA-DR in Akata$^-$ EBV-eGFP cells (top left) or caveolin-1 in Vero-E6 cells (bottom middle) under cocultured conditions. The bright-field images are shown (right). Scale bars, 100 μm. ERK is phosphorylated in cocultured Akata$^-$ EBV-eGFP (B) or Vero-E6 cells (C). Vero-E6 cells were cocultured with Akata$^-$ EBV-eGFP cells in the presence (b to e) or absence (f) of αhIgG for various times. The phosphorylation of ERK in Akata$^-$ EBV-eGFP (B) or Vero-E6 (C) cells was examined by immunofluorescent staining (top). The effect of U0126 treatment (0.2 μM) on the phosphorylation of ERK is shown in image e. As a control, the status of ERK phosphorylation in untreated Akata$^-$ EBV-eGFP or Vero-E6 cells is shown in image a. Bright-field images are shown at the bottom. Scale bars, 100 μm. (D) The percentages of the cells positive for the phosphorylation of ERK were analyzed by a confocal laser scanning microscope. The experiment was performed three times independently. The averages and standard deviations are shown for each condition. **, $P < 0.01$ versus the respective control (Student's *t* test).

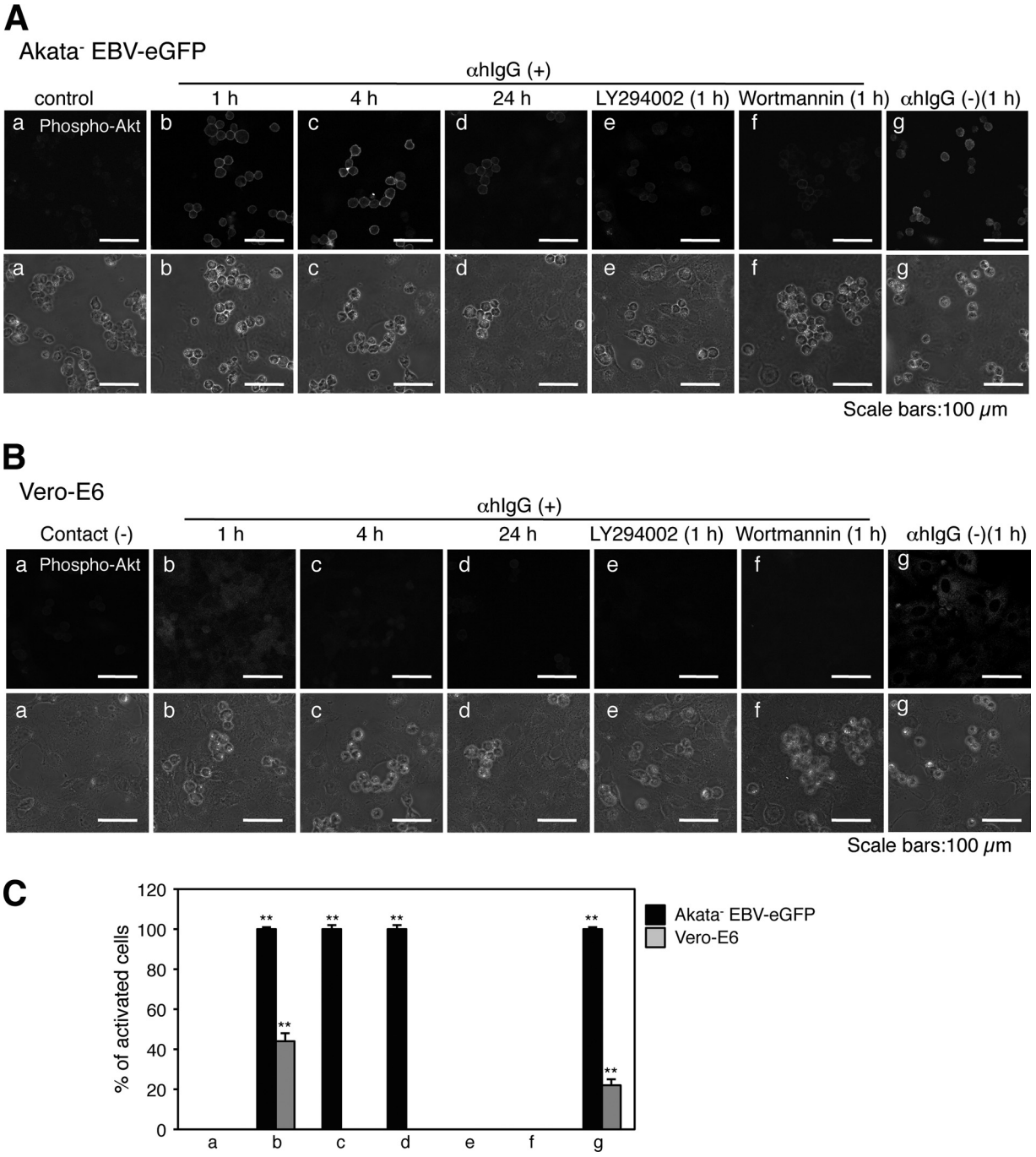

FIG 6 Activation of the PI3K pathway in cocultured cells. Akt is phosphorylated in cocultured Akata$^-$ EBV-eGFP (A) or Vero-E6 (B) cells. Vero-E6 cells were cocultured with Akata$^-$ EBV-eGFP cells in the presence (b to f) or absence (g) of αhIgG for various times. The phosphorylation of Akt in Akata$^-$ EBV-eGFP (A) or Vero-E6 (B) cells was examined by immunofluorescent staining (top). The effect of LY294002 treatment (0.2 μM) (e) or wortmannin treatment (0.1 μM) (f) on the phosphorylation of Akt is shown. As a control, the status of Akt phosphorylation in Akata$^-$ EBV-eGFP or Vero-E6 cells not treated with αhIgG is shown in image a. Bright-field images are shown (bottom). Scale bars, 100 μm. (C) The percentages of the cells exhibiting phosphorylation of Akt were analyzed by a confocal laser scanning microscope. The experiment was performed three times independently. The averages and standard deviations are shown for each condition. **, $P < 0.01$ versus the respective control (Student's *t* test).

nucleus in Akata$^-$ EBV-eGFP cells 24 h after cocultivation (Fig. 7A and C). Treatment with U0126, LY294002, wortmannin, or BAY11-7082 specifically blocked the activation of individual target molecules (Fig. 5 to 7). Interestingly, these signaling molecules were also activated in the cocultured cells in the absence of αhIgG (Fig. 5 to 7).

Cell-to-cell contact induces viral replication. We observed that EBV is transmitted to epithelial cells in the absence of αhIgG (Fig. 1A to C). The inhibitor treatments and the knockdown of RelA/p65 also reduced viral transmission and lytic induction in the absence of αhIgG (Fig. 4A and C). The signaling molecules were activated in the cocultured cells in the absence of αhIgG (Fig.

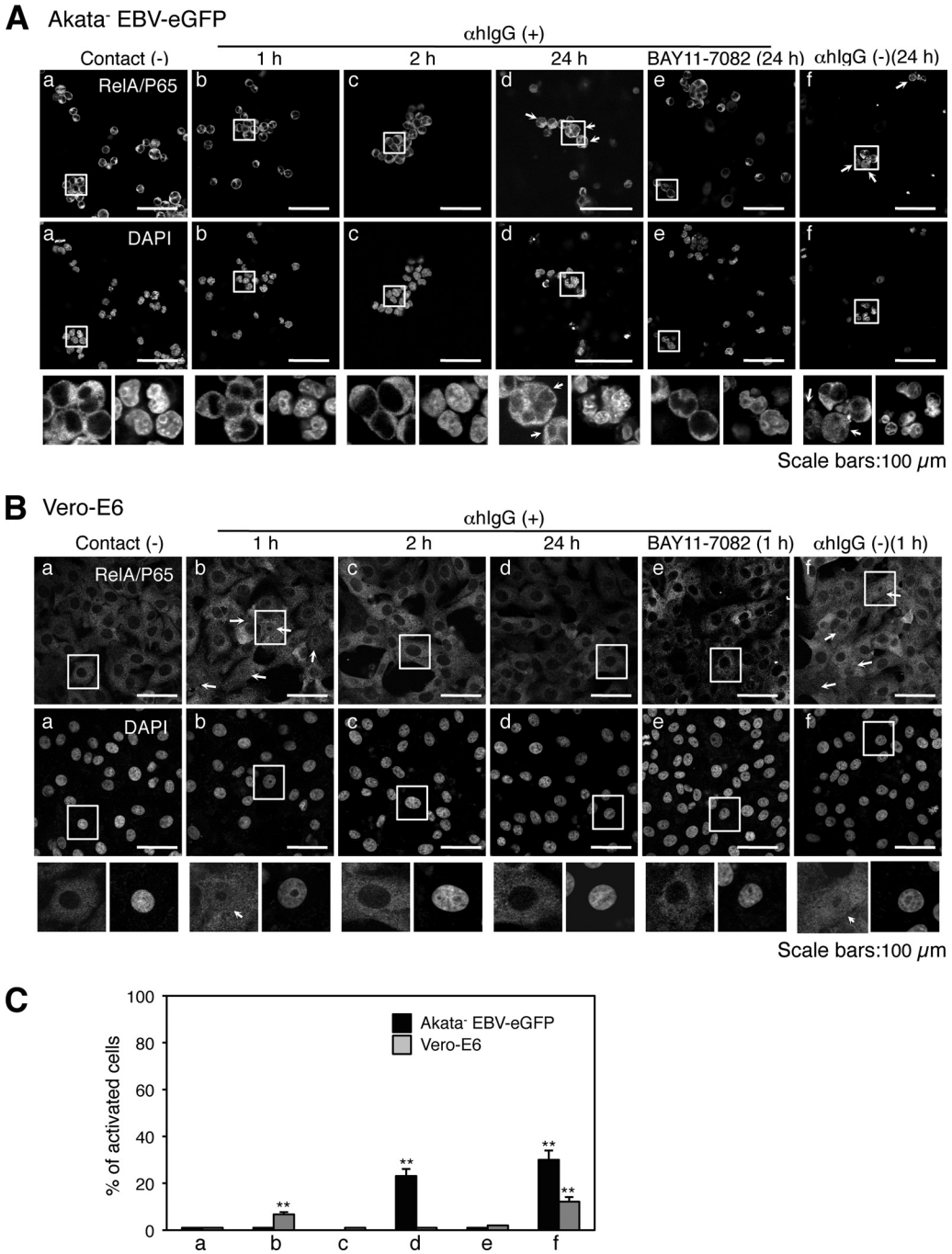

FIG 7 Activation of the NF-κB pathway in cocultured cells. The nuclear translocation of RelA/p65 in cocultured Akata$^-$ EBV-eGFP (A) or Vero-E6 (B) cells. Vero-E6 cells were cocultured with Akata$^-$ EBV-eGFP cells in the presence (b to e) or absence (f) of αhIgG for various times. The translocation of RelA/p65 in Akata$^-$ EBV-eGFP (A) or Vero-E6 (B) cells was examined by immunofluorescent staining (top). The effect of BAY11-7082 treatment (2 μM) on the translocation of RelA/p65 is shown in image e. As a control, the status of RelA/p65 translocation in Akata$^-$ EBV-eGFP or Vero-E6 cells not treated with αhIgG is shown in image a. The nucleus is counterstained with DAPI (bottom). Insets show enlargements of the boxed areas. Scale bars, 100 μm. (C) The percentages of the cells that contain the translocation of RelA/p65 were analyzed by a confocal laser scanning microscope. The experiment was performed three times independently. The averages and standard deviations are shown for each condition. **, $P < 0.01$ versus the respective control (Student's *t* test).

5A and 6A). Therefore, we tested whether cell-to-cell contact induces the viral lytic cycle in the latently infected Akata$^-$ EBV-eGFP cells and leads to viral transmission. We cocultured Vero-E6 cells with Akata$^-$ EBV-eGFP cells and analyzed the efficiencies of lytic induction in Akata$^-$ EBV-eGFP cells by FISH analyses using Cy3-labeled probe, which specifically hybridized to the EBV genome. The EBV genomes were significantly amplified (10^2- to 10^3-fold) in the nucleus under the treatment of αhIgG (Fig. 8A, bottom right). FISH analysis showed that less than 1% of the cell population underwent lytic induction without αhIgG treatment

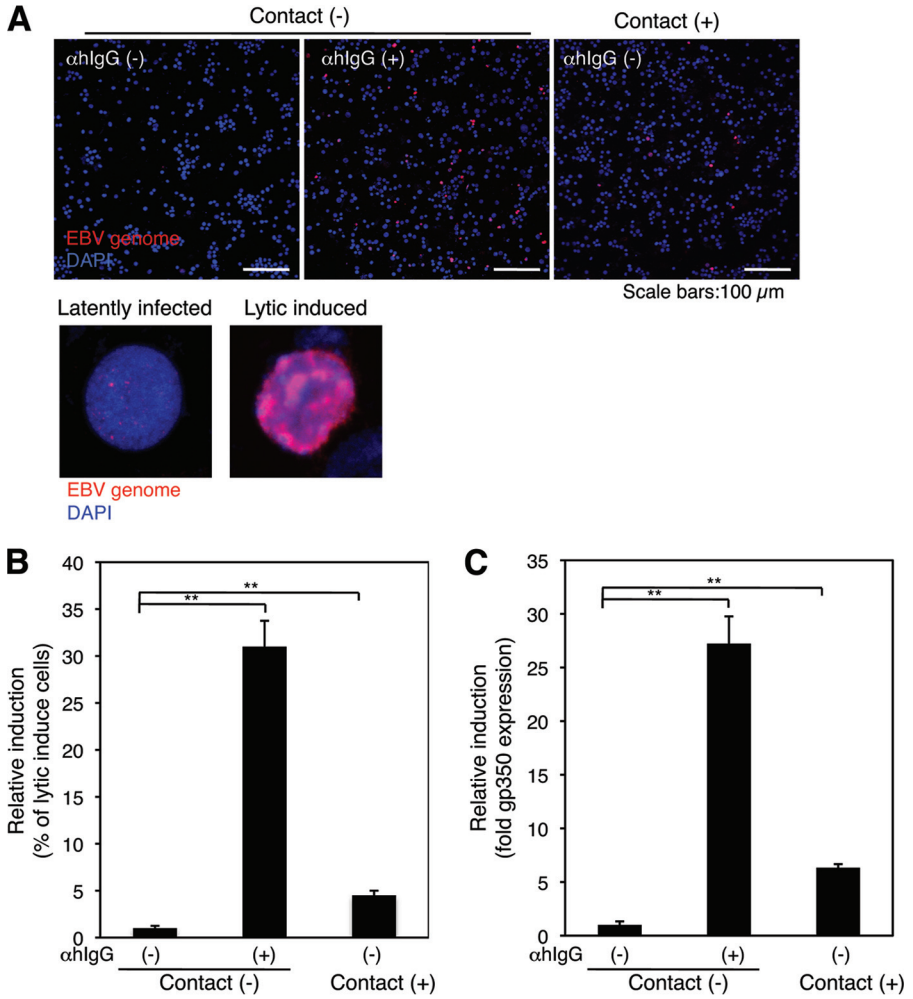

FIG 8 Lytic cycle is induced in cocultured BL cells. (A) Vero-E6 cells were cocultured with Akata$^-$ EBV-eGFP cells in the absence of αhIgG for 24 h (top, right). As a control, Akata$^-$ EBV-eGFP cells were treated in the presence (top middle) or absence of αhIgG (top left). Akata$^-$ EBV-eGFP cells were harvested, and the induction of the lytic cycle was analyzed by FISH using Cy3-labeled probe for the EBV genome (top). Enlarged images of the cell in latent (bottom left) or lytic (bottom right) phase are shown. The nucleus was counterstained with DAPI. Scale bars, 100 μm. (B) The percentages of Akata$^-$ EBV-eGFP cells undergoing the lytic cycle were analyzed by a confocal laser scanning microscope. The experiment was performed three times independently. The averages and standard deviations are shown for each condition. **, $P < 0.01$ versus the respective control (Student's *t* test). (C) The expression of gp350 in cocultured BL cells. The expression of gp350 was analyzed by flow cytometry. The experiment was performed three times independently. The averages and standard deviations are shown for each condition. **, $P < 0.01$ versus the respective control (Student's *t* test).

(Fig. 8A, top left, and B). By αhIgG treatment, 12% of Akata$^-$ EBV-eGFP cells underwent the lytic cycle (Fig. 8A, top middle, and B). The rate of lytic induction in Akata$^-$ EBV-eGFP cells increased by up to 2% by cocultivation with Vero-E6 cells (Fig. 8A, top right, and B), indicating that cell-to-cell contact between BL cells latently infected with EBV and epithelial cells initiated lytic induction. Immunofluorescent staining analysis also demonstrated that gp350 expression was enhanced in Akata$^-$ EBV-eGFP cells by cocultivation with Vero-E6 cells (Fig. 8C).

DISCUSSION

In the present study, we demonstrated the roles of the cell signaling pathways in cell-to-cell contact-mediated EBV transmission by using an *in vitro* cocultivation system. Our observations indicate that (i) cell-to-cell contact without cell-to-cell fusion contributes to viral transmission (Fig. 1 to 3); (ii) the treatment of inhibitors of the ERK and NF-κB pathways downregulates EBV transmission in addition to lytic induction, blockage of the PI3K pathway impairs EBV transmission coupled with the inhibition of the lytic induction, and the knockdown of RelA/p65 significantly downregulates cell-to-cell contact-mediated viral transmission (Fig. 4); (iii) the ERK, PI3K, and NF-κB pathways are activated in cocultured BL and epithelial cells (Fig. 5 to 7); and (iv) cell-to-cell contact initiates the induction of the lytic cycle in BL cells (Fig. 8).

αhIgG treatment amplified EBV transmission into epithelial cells (Fig. 1A, B, and D), indicating that the synthesis of progeny virus in Akata$^-$ EBV-eGFP cells is indispensable for cell-to-cell viral transmission. It has been reported that a small fraction of Akata cells (1%) spontaneously enters into the lytic cycle (41) (Fig. 8A, left). By cocultivation with Vero-E6 cells, the viral lytic cycle was induced in Akata$^-$ EBV-eGFP cells (Fig. 8A, middle, and B) in the absence of αhIgG, suggesting that the cell-to-cell contact-mediated lytic induction contributes to viral transmission into the epithelial cells under physiological conditions. It has been shown

that a variety of signal transductions, including the ERK and PI3K pathways, are synergistically activated during the EBV lytic cycle (18). We showed that the specific inhibitors of the ERK and PI3K pathways blocked EBV replication (Fig. 4A, bottom) and that ERK and Akt were phosphorylated in cocultured Akata$^-$ EBV-eGFP cells in the absence of αhIgG treatment (Fig. 5 and 6). These data suggest that the activation of the ERK and PI3K pathways contributes to cell-to-cell contact-mediated viral lytic induction in Akata$^-$ EBV-eGFP cells. It is known that the EBV-encoded immediate-early protein ZTA, which is important for the switch to viral lytic replication, is inhibited by the RelA/p65 subunit (4, 25). However, no enhancement of EBV replication was observed under BAY11-7082 treatment in our study (Fig. 4, bottom). The discrepancy may result from a difference in the experimental systems (e.g., single cultured B cells versus cocultured B cells). The NF-κB pathway was activated in Akata$^-$ EBV-eGFP cells in the late stage of cell-to-cell contact-mediated EBV transmission (Fig. 7A and C). The role of the NF-κB pathway in B cells in cell-to-cell contact-mediated EBV transmission remains unclear, and its further investigation is required.

Shannon-Lowe and colleagues have demonstrated that EBV virions loaded on the surface of primary B cells facilitate the formation of a virological synapse (VS)-like intercellular conjugation between B cells and cocultured epithelial cells (34, 35). The VS is a tight adhesive junction across which virus can be efficiently transferred from virus-infected cells to noninfected target cells without cell-cell fusion. The VS has been intensively studied in the field of retroviruses (17). The ERK pathway appears to enhance the polarization of the mitotic organizing center (MTOC) and contributes to microtubule-dependent trafficking of viral Gag proteins (29). We demonstrated that an ERK inhibitor, U0126, significantly blocked EBV transmission with a partial impairment of induction of the lytic cycle (Fig. 4A), and that ERK was phosphorylated in cocultured Akata$^-$ EBV-eGFP cells (Fig. 5A). These observations suggest that the ERK pathway plays a role in the efficient trafficking of EBV virions to the intercellular space mediated by MTOC polarization.

We also demonstrated that the PI3K and NF-κB pathways contribute to viral transmission (Fig. 4). Previous observations have demonstrated an important role of an EBV glycoprotein, BMRF-2, in the cell-to-cell spread of EBV in polarized oral epithelial cells (47, 48). BMRF-2 interacts with β1 and αv integrins and initiates PI3K signaling, events that are crucial for the entry of EBV into B cells (10). NF-κB signaling is activated by the conjugation of viral gp350/200 with CD21 in B cells (8, 38). It is possible that the binding of BMRF-2 to the integrins and that of gp350/200 to undefined viral receptors in epithelial cells trigger the PI3K and NF-κB pathways and promote entry of intercellular EBV virions into adjacent epithelial cells. We demonstrated that the phosphorylation of Akt and the nuclear translocation of RelA/p65 were induced in Vero-E6 cells 1 h after cocultivation (Fig. 6B and C). The expression of viral glycoproteins and the generation of progeny virions are unlikely to be induced by 1 h after cell-to-cell contact-mediated lytic induction. The roles of PI3K and NF-κB in the processes of EBV entry into epithelial cells mediated by cell-to-cell contact currently remain unknown and warrant further investigation.

In our study, we used a monkey and two human epithelial cell lines as recipient cells. It would be interesting and informative to test our findings in EBV-negative primary human epithelial cells in the future.

Taken together, this study provides a tractable system to examine cell-to-cell transmission of EBV to epithelial cells. Our observations indicate that multiple intracellular signaling molecules play roles in cell-to-cell contact-mediated EBV transmission and serve as a basis to understand better the mechanism of cell-to-cell viral transmission.

ACKNOWLEDGMENTS

We thank Ayato Takada (Hokkaido University), Kenji Oritani (Osaka University), and Hironori Yoshiyama (Hokkaido University) for providing us with Vero-E6 cells, PE-labeled anti-human HLA-DR antibody, and anti-EBNA1 polyclonal antibody, respectively. We also thank Bill Sugden (University of Wisconsin, Madison) and Yusuke Ohba (Hokkaido University) for critically reviewing the manuscript.

This work was supported by grants in aid from the Japanese Ministry of Education, Science, Sports, Culture, and Technology, Japan.

REFERENCES

1. **Akiyama S, et al.** 1988. Characteristics of three human gastric cancer cell lines, NU-GC-2, NU-GC-3 and NU-GC-4. Jpn. J. Surg. **18**:438–446.
2. **Barranco SC, et al.** 1983. Establishment and characterization of an in vitro model system for human adenocarcinoma of the stomach. Cancer Res. **43**:1703–1709.
3. **Boulton TG, et al.** 1991. ERKs: a family of protein-serine/threonine kinases that are activated and tyrosine phosphorylated in response to insulin and NGF. Cell **65**:663–675.
4. **Brown HJ, et al.** 2003. NF-kappaB inhibits gammaherpesvirus lytic replication. J. Virol. **77**:8532–8540.
5. **Chang Y, et al.** 1999. Requirement for cell-to-cell contact in Epstein-Barr virus infection of nasopharyngeal carcinoma cells and keratinocytes. J. Virol. **73**:8857–8866.
6. **Connolly SA, Jackson JO, Jardetzky TS, Longnecker R.** 2011. Fusing structure and function: a structural view of the herpesvirus entry machinery. Nat. Rev. Microbiol. **9**:369–381.
7. **Couet J, Belanger MM, Roussel E, Drolet MC.** 2001. Cell biology of caveolae and caveolin. Adv. Drug Deliv. Rev. **49**:223–235.
8. **DE Oliveira DE, Ballon G, Cesarman E.** 2010. NF-kappaB signaling modulation by EBV and KSHV. Trends Microbiol. **18**:248–257.
9. **Desmyter J, Melnick JL, Rawls WE.** 1968. Defectiveness of interferon production and of rubella virus interference in a line of African green monkey kidney cells (Vero). J. Virol. **2**:955–961.
10. **Dorner M, et al.** 2010. Beta1 integrin expression increases susceptibility of memory B cells to Epstein-Barr virus infection. J. Virol. **84**:6667–6677.
11. **Favata MF, et al.** 1998. Identification of a novel inhibitor of mitogen-activated protein kinase kinase. J. Biol. Chem. **273**:18623–18632.
12. **Fingeroth JD, Diamond ME, Sage DR, Hayman J, Yates JL.** 1999. CD21-dependent infection of an epithelial cell line, 293, by Epstein-Barr virus. J. Virol. **73**:2115–2125.
13. **Hutt-Fletcher LM.** 2007. Epstein-Barr virus entry. J. Virol. **81**:7825–7832.
14. **Iankov ID, et al.** 2006. Immunoglobulin G antibody-mediated enhancement of measles virus infection can bypass the protective antiviral immune response. J. Virol. **80**:8530–8540.
15. **Imai S, Nishikawa J, Takada K.** 1998. Cell-to-cell contact as an efficient mode of Epstein-Barr virus infection of diverse human epithelial cells. J. Virol. **72**:4371–4378.
16. **Iwakiri D, Eizuru Y, Tokunaga M, Takada K.** 2003. Autocrine growth of Epstein-Barr virus-positive gastric carcinoma cells mediated by an Epstein-Barr virus-encoded small RNA. Cancer Res. **63**:7062–7067.
17. **Jolly C, Sattentau QJ.** 2004. Retroviral spread by induction of virological synapses. Traffic **5**:643–650.
18. **Kenney SC.** 2007. Reactivation and lytic replication of EBV. *In* Arvin A, et al (ed), Human herpesviruses: biology, therapy, and immunoprophylaxis, chapter 25. Cambridge University Press, Cambridge, United Kingdom.
19. **Kieff E, Rickinson AB.** 2001. Epstein-Barr virus and its replication, p 2511–2573. *In* Knipe DM, et al (ed), Fields virology, 4th ed. Lippincott Williams & Wilkins, Philadelphia, PA.
20. **Klein E, et al.** 1968. Surface IgM-kappa specificity on a Burkitt lymphoma cell in vivo and in derived culture lines. Cancer Res. **28**:1300–1310.

21. **Liu P, Cheng H, Roberts TM, Zhao JJ.** 2009. Targeting the phosphoinositide 3-kinase pathway in cancer. Nat. Rev. Drug Discov. **8**:627–644.
22. **Maruo S, Yang L, Takada K.** 2001. Roles of Epstein-Barr virus glycoproteins gp350 and gp25 in the infection of human epithelial cells. J. Gen. Virol. **82**:2373–2383.
23. **Mattioli I, et al.** 2004. Transient and selective NF-kappa B p65 serine 536 phosphorylation induced by T cell costimulation is mediated by I kappa B kinase beta and controls the kinetics of p65 nuclear import. J. Immunol. **172**:6336–6344.
24. **McShane MP, Longnecker R.** 2004. Cell-surface expression of a mutated Epstein-Barr virus glycoprotein B allows fusion independent of other viral proteins. Proc. Natl. Acad. Sci. U. S. A. **101**:17474–17479.
25. **Mothes W, Sherer NM, Jin J, Zhong P.** 2010. Virus cell-to-cell transmission. J. Virol. **84**:8360–8368.
26. **Nanbo A, et al.** 2010. Ebolavirus is internalized into host cells via macropinocytosis in a viral glycoprotein-dependent manner. PLoS Pathog. **6**:e1001121. doi:10.1371/journal.ppat.1001121.
27. **Nanbo A, Sugden A, Sugden B.** 2007. The coupling of synthesis and partitioning of EBV's plasmid replicon is revealed in live cells. EMBO J. **26**:4252–4262.
28. **Nanbo A, Yoshiyama H, Takada K.** 2005. Epstein-Barr virus-encoded poly(A)-RNA confers resistance to apoptosis mediated through Fas by blocking the PKR pathway in human epithelial intestine 407 cells. J. Virol. **79**:12280–12285.
29. **Nejmeddine M, et al.** 2009. HTLV-1-Tax and ICAM-1 act on T-cell signal pathways to polarize the microtubule-organizing center at the virological synapse. Blood **114**:1016–1025.
30. **Nemerow GR, Mold C, Schwend VK, Tollefson V, Cooper NR.** 1987. Identification of gp350 as the viral glycoprotein mediating attachment of Epstein-Barr virus (EBV) to the EBV/C3d receptor of B cells: sequence homology of gp350 and C3 complement fragment C3d. J. Virol. **61**:1416–1420.
31. **Nishikawa J, et al.** 1999. Epstein-Barr virus promotes epithelial cell growth in the absence of EBNA2 and LMP1 expression. J. Virol. **73**:1286–1292.
32. **Oda T, Imai S, Chiba S, Takada K.** 2000. Epstein-Barr virus lacking glycoprotein gp85 cannot infect B cells and epithelial cells. Virology **276**:52–58.
33. **Omerovic J, Lev L, Longnecker R.** 2005. The amino terminus of Epstein-Barr virus glycoprotein gH is important for fusion with epithelial and B cells. J. Virol. **79**:12408–12415.
34. **Shannon-Lowe C, Rowe M.** 2011. Epstein-Barr virus infection of polarized epithelial cells via the basolateral surface by memory B cell-mediated transfer infection. PLoS Pathog. **7**:e1001338. doi:10.1371/journal.ppat.1001338.
35. **Shannon-Lowe CD, Neuhierl B, Baldwin G, Rickinson AB, Delecluse HJ.** 2006. Resting B cells as a transfer vehicle for Epstein-Barr virus infection of epithelial cells. Proc. Natl. Acad. Sci. U. S. A. **103**:7065–7070.
36. **Sinclair AJ, Farrell PJ.** 1995. Host cell requirements for efficient infection of quiescent primary B lymphocytes by Epstein-Barr virus. J. Virol. **69**:5461–5468.
37. **Speck P, Longnecker R.** 2000. Infection of breast epithelial cells with Epstein-Barr virus via cell-to-cell contact. J. Natl. Cancer Inst. **92**:1849–1851.
38. **Sugano N, Chen W, Roberts ML, Cooper NR.** 1997. Epstein-Barr virus binding to CD21 activates the initial viral promoter via NF-kappaB induction. J. Exp. Med. **186**:731–737.
39. **Takada K.** 1984. Cross-linking of cell surface immunoglobulins induces Epstein-Barr virus in Burkitt lymphoma lines. Int. J. Cancer **33**:27–32.
40. **Takada K, et al.** 1991. An Epstein-Barr virus-producer line Akata: establishment of the cell line and analysis of viral DNA. Virus Genes **5**:147–156.
41. **Takada K, Ono Y.** 1989. Synchronous and sequential activation of latently infected Epstein-Barr virus genomes. J. Virol. **63**:445–449.
42. **Tao Q, et al.** 1995. Evidence for lytic infection by Epstein-Barr virus in mucosal lymphocytes instead of nasopharyngeal epithelial cells in normal individuals. J. Med. Virol. **45**:71–77.
43. **Tao Q, Srivastava G, Chan AC, Ho FC.** 1995. Epstein-Barr-virus-infected nasopharyngeal intraepithelial lymphocytes. Lancet **345**:1309–1310.
44. **Thorley-Lawson DA, Geilinger K.** 1980. Monoclonal antibodies against the major glycoprotein (gp350/220) of Epstein-Barr virus neutralize infectivity. Proc. Natl. Acad. Sci. U. S. A. **77**:5307–5311.
45. **Trowsdale J, Ragoussis J, Campbell RD.** 1991. Map of the human MHC. Immunol. Today **12**:443–446.
46. **Walker EH, et al.** 2000. Structural determinants of phosphoinositide 3-kinase inhibition by wortmannin, LY294002, quercetin, myricetin, and staurosporine. Mol. Cell **6**:909–919.
47. **Xiao J, Palefsky JM, Herrera R, Berline J, Tugizov SM.** 2009. EBV BMRF-2 facilitates cell-to-cell spread of virus within polarized oral epithelial cells. Virology **388**:335–343.
48. **Xiao J, Palefsky JM, Herrera R, Berline J, Tugizov SM.** 2008. The Epstein-Barr virus BMRF-2 protein facilitates virus attachment to oral epithelial cells. Virology **370**:430–442.
49. **Yoshiyama H, Imai S, Shimizu N, Takada K.** 1997. Epstein-Barr virus infection of human gastric carcinoma cells: implication of the existence of a new virus receptor different from CD21. J. Virol. **71**:5688–5691.
50. **Zanotto-Filho A, et al.** 2010. The pharmacological NFkappaB inhibitors BAY117082 and MG132 induce cell arrest and apoptosis in leukemia cells through ROS-mitochondria pathway activation. Cancer Lett. **288**:192–203.